EFFECTS OF GRAPHENE OXIDE WITH DIFFERENT OXIDATION DEGREE ON THE PROPERTIES OF EPOXY NANOCOMPOSITES

Xiaoyu Hu[1], Wanshuang Liu*[1], Yi Wei[1]

[1] Donghua University Center for Civil Aviation Composites, Donghua University, 2999 North Renmin Road, Shanghai, 201620, China. Emal: wsliu@dhu.edu.cn.
Website: http://texcol.dhu.edu.cn/4a/7f/c6551a150143/page.htm

Keywords: Graphene oxide, Oxidation degree, Polymer-matrix composites, Epoxy toughening

ABSTRACT

In this work, five graphene oxide (GO) with different oxidation degree were prepared *via* a modified Hummers' method by varying the oxidant/graphite ratio and oxidation time. The structure evolution of GO with the development of oxidation was investigated by X-ray photoelectron spectroscopy, Fourier transform infrared spectroscopy, Raman spectroscopy, and X-ray diffraction measurements. The prepared GO powders were used to reinforced epoxy resin, and the surfaces of GO can be functionalized by the amine hardener during the dispersion process. Microscopic observations show that the oxidation degree of GO greatly affects the dispersion state of GO in the epoxy matrix. The GO samples with the lowest and highest oxidation degree tend to aggregate. The GO sample with optimized structure (GO-4) shows superior toughening effects on the epoxy matrix compared with the epoxy/GO composites in the previous reports. The addition of 0.2 wt% GO-4 can yield 56 and 128% enhancement the critical stress intensity factor (K_{IC}) and the critical strain energy release rate (G_{IC}), respectively.

1 INTRODUCTION

Epoxy resins, a class of important thermoset polymer, have been widely used in many applications, including protective coatings, versatile adhesives, electronic encapsulating materials and polymer matrices for fiber reinforced composites [1]. Epoxy resins have an excellent combination of good mechanical properties, dimensional stability, heat and chemical resistance due to their highly crosslinked network structures. However, this feature makes epoxy resins intrinsically brittle and show poor resistance to crack propagation, which limits their application at the frontier of many industrial fields [2]. Therefore, intensive research efforts have been devoted to toughening of brittle epoxy polymers over the last few decades. A traditional strategy is to introduce high toughness modifiers like liquid rubbers [3-5] and thermoplastic polymers into epoxy matrix [6-9]. The microphase of modifiers formed during the curing process can initiate various toughening mechanisms such as matrix shear banding, debonding/cavitation of modifiers, matrix void growth, crack bridging and deflection [3-9]. Although the toughening effects of rubbers and thermoplastic polymers are significant, the high loadings (5-20 wt%) of these soft modifiers can distinctly reduce the stiffness, strength, and glass transition temperature of epoxy matrix. To address these issues, inorganic fillers with high stiffness have also been investigated as another class of toughening modifiers. Unlike polymeric modifiers, the incorporation of inorganic fillers can increase the fracture toughness of epoxy matrix without any significant reduction in modulus and glass transition temperature [10,11]. So far various inorganic fillers, such as silica [12], clay [13], carbon nanotubes [14], carbon nanofibers [15], graphene and its derivatives [16-18] have been used to toughen epoxy resins.

Graphene oxide (GO), an oxidized graphene derivative, has fascinating mechanical, chemical, optical and electrical properties [19]. As a reinforcing filler for polymer composites, GO even has many advantages over graphene due to the existence of various reactive oxygen-containing functional groups. These functional groups can facilitate the dispersion of GO in some polar polymer matrices and provide a platform for further surface modification [20]. GO has proven to be an effective nanofiller for epoxy toughening [17,21-25]. However, it is noteworthy that the toughening effects of GO on epoxy resins in previous reports are quite different. Compared with neat epoxy sample, the

reported maximum increase in critical stress intensity factor (K_{IC}) for epoxy/GO composites ranged from 19 to 63 % [17,21-25]. It's known that the mechanical performance of GO reinforced epoxy resins depends greatly on the dispersion state of GO and the extent of interfacial interactions. These two factors are both related to the structure of GO, i.e. the oxygen-containing functional groups on GO surface. Therefore, the regulation of surface chemistry of GO would contribute to optimizing its reinforcing efficiency. To the best of our knowledge, the relationship between GO structure and its toughening effects on epoxy resins has rarely been investigated.

In this study, we aim to provide a better understanding of the effects of GO structure on the properties of epoxy/GO composites. First, five GO powders with different oxidation degree were prepared through a modified Hummers' method by changing the oxidation conditions. The structure evolution of GO was investigated as the oxidation developed. Typical bisphenol A epoxy/amine system was used as resin matrix, and the surfaces of GO were functionalized during the dispersion process *via* the reactions between GO and the amine hardener. The dispersibility of various GO in the epoxy matrix was investigated by optical microscope and transmission electron microscopy (TEM). The influences of GO structure on the curing behaviors, rheological, thermal and mechanical properties of epoxy matrix were systematically investigated. Emphasis is placed on the effects of GO structure on the fracture toughness of the resulting composites, and the reinforcing efficiency of GO in this work was compared with the reported epoxy/GO composites.

2 EXPERIMENTAL

2.1. Materials

Graphite flake (99.9 %, -10 mesh) was supplied by Alfa Aesar (USA). Epoxy 5417A (a bisphenol A type epoxy) with an epoxy equivalent weight of 165–175 was supplied by Wells Advanced Materials Co., Ltd. (China). Isophoronediamine (IPDA, 99 %) was purchased from J&K Chemicals Inc. (China). Sulfuric acid (H_2SO_4, 95-97 %), sodium nitrate ($NaNO_3$), hydrogen peroxide (H_2O_2, 30%), and potassium permanganate ($KMnO_4$) were purchased from Sinopharm Chemical Reagent Co., Ltd. (China).

2.2. Preparation of GO with different oxidation degree

GO was prepared from natural graphite flakes *via* a modified Hummers method. Typically, graphite (1.0 g) and sodium nitrate ($NaNO_3$, 1.0 g) were mixed with sulfuric acid (H_2SO_4, 48 mL) in a 250 mL flask. The mixture was stirred and kept at ~0 °C for 15 min in an ice bath. Then, potassium permanganate ($KMnO_4$, 3.0 g) was slowly added to the mixture in 30 min under continuous stirring. The ice bath was removed and the mixture was stirred at 45 °C for 3 h. Afterwards, deionized (DI) water (60 mL) was slowly added to the pasty mixture under vigorous stirring. The mixture temperature rapidly increased to over 90 °C with effervescence. After 30 min, DI water (100 mL) and hydrogen peroxide (H_2O_2, 5 mL) were added to finish the reaction. For preliminary purification, the obtained light yellow mixture was first washed with 5% hydrochloric acid (HCl), followed by DI water for three times to remove residual acid and metal ions. Then, the mixture is centrifuged for 15 min at 10,000 rpm. The obtained brown GO powders were freeze-dried for 48 h and stored in ambient environment.

GO powders with different oxidation degree (GO-1 to GO-5) were prepared by varying the potassium permanganate/graphite ratio and reaction time. The preparation conditions of different GO samples are summarized in Table 1. Double volume of H_2SO_4 was used for GO-5, otherwise the mixture became quite thick and could not be stirred after ~10 h.

2.3. Preparation of epoxy/GO composites

A desired amount of GO powder was firstly dispersed into IPDA by high-speed shear mixing (3000 rpm) for 30 min using a homogenizer. To avoid overheating, the mixing process was conducted intermittently (10 min on and 10 min off). The obtained mixture was further sonicated in an ultrasonic water bath for 30 min, followed by magnetic stirring at 90 °C for 6h. After cooling down to the room temperature, a calculated quality of epoxy 5417A (mole ratio of epoxy group to amino group was 2:1)

was added and mechanically mixed together. After degassing, the resulting epoxy/GO mixture was poured into aluminum molds with specific dimensions for mechanical tests. Finally, the samples were cured at 60 °C for 2h and post-cured at 140 °C for 4 h. As a control, neat epoxy/IPDA sample was also prepared under the same condition.

Table 1 Experimental parameters for GO preparation.

Sample	Graphite (g)	$KMnO_4$ (g)	$NaNO_3$ (g)	H_2SO_4 (mL)	time (h)
GO-1	1.0	1.0	1.0	48	3
GO-2	1.0	3.0	1.0	48	3
GO-3	1.0	6.0	1.0	48	3
GO-4	1.0	6.0	1.0	48	6
GO-5	1.0	6.0	1.0	96	12

2.4. Characterization

Elemental analysis was conducted on an Elementar Vario ELIII analyzer. The weight percentages of hydrogen, carbon, nitrogen and sulfur elements were measured. FTIR spectra were recorded on a Nicolet 6700 FTIR spectrometer using attenuated total reflection (ATR) mode. XPS measurements were conducted on a PE PHI-5300 ESCA system equipped with a monochromatized Cu Kα X-ray source. Raman spectra were recorded on a Renishaw InVia-Reflex Raman microscope using a 633 nm laser source. XRD measurement was performed on a HD-D/Max2550VB+/PC instrument. Dynamic mechanical analysis (DMA) for cured epoxy resins and composites was performed on a TA DMA Q800 at a frequency of 1 Hz and a heating rate of 3 °C min^{-1}.

Tensile properties were measured on an Instron Tester 5567 with a 2 kN load cell at a crosshead speed of 1 mm min^{-1}, following ASTM D-638 standard (sample type V). Fracture toughness of each sample was measured according to ASTM D5045 standard using a single-edge-notch bending geometry. A wedge-shape notch was accurately machined at the midpoint of each specimen using a band saw. A natural pre-crack was then introduced by slightly tapping a chilled blade (GEM) in the notch. The tests were conducted on an Instron Tester 5567 with a 500 N load cell at a crosshead speed of 10 mm min^{-1}. Critical stress intensity factor (K_{IC}) and critical strain energy release rate (G_{IC}) were calculated following the equations given in ASTM D 5045 standard. Each reported value for tensile and fracture toughness tests was the average of at least five valid specimens.

The disperse states of GO in epoxy matrices were inspected on an Olympus CK41 optical microscope. The morphologies of fracture surfaces from tensile tests were observed on a Hitachi S4800 scanning electron microscope (SEM). The samples were coated with gold for 100 s. Transmission electron microscopy (TEM) was performed on a JEOL JEM-2100 with a 200 kV accelerating voltage.

3 RESULTS AND DISCUSSION

3.1 Structure characterization and morphologies of GO

The compositions of five GO samples were studied by elemental analysis measurement and the results are summarized in Table 2. As can be seen, the preparation conditions indeed have a distinct impact on the compositions of GO. With increasing the quantity of oxidant and reaction time, the oxygen and hydrogen contents of GO continuously increase from 31.2 and 1.5 wt% to 46.9 and 2.9 wt%, respectively, whereas the carbon content decreases from 67.3 to 49.7 wt%. It should be noted that the oxidation degree of GO shows a significant increase as the oxidant/graphite ratio increases from 1 to 3 (GO-1 and GO-2). Another large increase in oxidation degree is observed when the reaction time extends from 6 h to 12 at a high oxidant/graphite ratio (GO-4 and GO-5).

XPS is a powerful tool to investigate the chemical compositions and structure of functional groups on the surface of GO. The compositions of GO measured by XPS are shown in Table 2. As can be seen, the oxygen contents on the surface of various GO follow the same trend with the results of

elemental analysis. From GO-1 to GO-5, the C/O atom ratio shows a decrease from 2.3 to 1.5. A tiny amount of nitrogen and sulfur elements were also detected on the surface of GO, which may come from the residual of sodium nitrate and sulfuric acid.

Table 2 Summary of elemental analysis and XPS data

Sample	Elemental analysis					XPS			
	C (wt%)	H (wt%)	O (wt%)	N (wt%)	S (wt%)	C (at%)	O (at%)	N (at%)	S (at%)
GO-1	67.3	1.5	31.2	-	-	67.7	29.4	1.7	1.2
GO-2	59.1	2.1	38.8	-	-	64.9	33.1	0.9	1.1
GO-3	57.5	2.3	40.2	-	-	62.9	34.4	1.4	1.3
GO-4	54.0	2.7	43.1	-	0.2	59.1	36.4	1.6	2.9
GO-5	49.7	2.9	46.9	-	0.5	57.9	37.5	1.4	3.2

To gain more insight, the structure evolution of various GO was also studied by FTIR spectroscopy (Fig. 1a). From the FTIR spectra of GO, the broad band between 3600-2000 cm^{-1} can be attributed to the O-H (carboxyl, phenolic and aliphatic hydroxyl groups) stretching vibrations. The band at 1715 cm^{-1} can be assigned to the overlap of C=O stretching vibrations from carboxyl, ketone and lactone groups. The bands at 1620, 1400 and 1225 cm^{-1} are related to C=C stretching, O-H bending and C-O (phenolic and carboxyl groups) stretching vibrations, respectively. The bands at 1150, 1040 and 865 cm^{-1} can be attributed to C-O-C (epoxy/ether groups) stretching, C-O (aliphatic hydroxyl group) stretching, and C-O-C (epoxy) asymmetric stretching vibrations.

The oxidation mechanism of GO is still uncertain due to its nonstoichiometric atomic composition. According to oxidation mechanism proposed by Kosynkin, the permanganate ion in acid media firstly broke the graphitic carbon layer, and carbonyl groups were formed. The carbonyl groups at the open edge can be further oxidized to carboxyl groups (Fig. 1b). With the enlarging open of graphite aroused by permanganate attack, oxygen-containing groups, such as phenolic, epoxy/ether and ketone groups, formed both on the basal plane and edges of graphene sheets. As the oxidation developed, more exposed graphene surfaces were oxidized, and phenolic groups converted to epoxy/ether, aliphatic hydroxyl, quinone, ketone or lactone groups (Fig. 1c). In this work, the FTIR spectrum of GO-1 shows significant absorption bands related with aromatic carbon, carboxyl, carbonyl and hydroxyl (phenolic and aliphatic) groups, whereas the bands related to epoxy/ether groups are relatively weak. With the increase in oxidation degree, the intensity of bands related to aromatic carbon and phenolic groups decreases, and the bands from epoxy/ether and aliphatic hydroxyl groups gradually become dominant (Fig. 1a), which is due to further oxidation of graphene surface and etherification of hydroxyl groups.

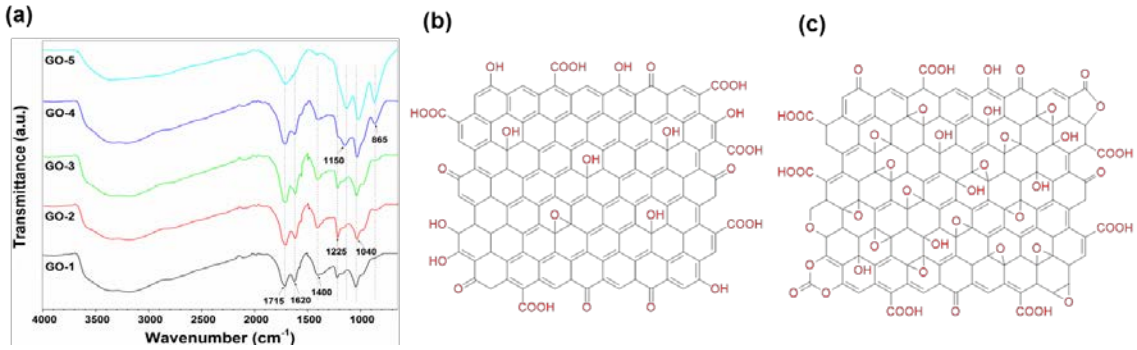

Figure 1: FTIR spectra of various GO samples (a); structural models of GO with low (b) and high (c) oxidation degree.

The structures of GO were further investigated by XRD and Raman spectroscopy. Fig.2 shows the XRD patterns of GO with different oxidation degree. GO-1 shows an intensive graphite peak (002) at 2 theta of 25° and a weak GO peak (002) at 2 theta of 9.6°, indicating the existence of large graphitic domains. As the oxidation degree increases, the intensity of graphite peak decreases and GO peak

becomes dominant. It should be noted that graphitic domain still exists on GO surface even at high oxidation degree. The interplanar distances (*d*) were calculated by Bragg law. Compared with GO-2, the *d* spacing of GO-3 decreases from 0.90 to 0.84 nm. GO-4 shows the maximum *d* spacing of 0.93 nm, whereas the *d* spacing of GO-5 decreases again down to 0.89 nm. These results indicate that the interplanar distance of GO depends on not only the quantity of oxygen-containing groups on GO sheets, but also the interactions between functional groups on adjacent GO sheets, such as hydrogen bonding.

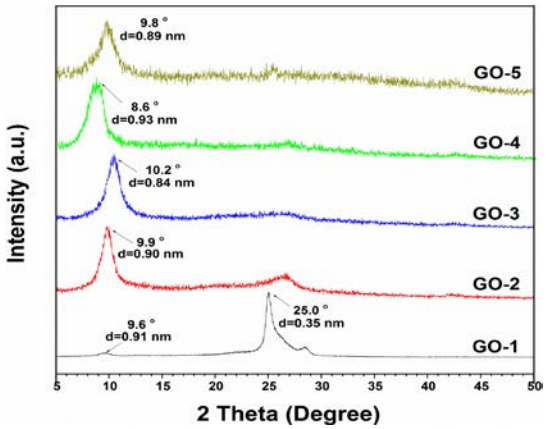

Figure 2: XRD patterns of GO-1, GO-2, GO-3, GO-4 and GO-5.

Raman spectroscopy can give insight into structural information of graphene-based materials, such as defects, disorder, layer number and crystallite size. Figs. 3a-e shows the typical Raman spectra of various GO samples. Four bands associated with D band (~1340 cm^{-1}), G band (~1600 cm^{-1}), 2D band (~2650 cm^{-1}) and D+G band (~2920 cm^{-1}) can be observed for all the GO samples. The D band can be ascribed to the A_{1g} phonon breathing vibrations from disordered carbon, and the G band is related to the E_{2b} mode of phonon vibrations from graphitic sp^2 hybridized carbon. The intensity ratios of the D band to G band (I_D/I_G) can indirectly reflect the oxidation degree of GO. In agreement with the results of FTIR spectroscopy, the values of I_D/I_G show continuous increase (Fig. 3f) from GO-1 to GO-5, indicating the increase in oxidation degree. In addition, the intensity ratios of I_{2D}/I_G is proportional to the layer number of GO, and the values decrease continuously from GO-1 to GO-5, (Fig. 3f) which indicates the increased exfoliation degree of graphite as the oxidation developed.

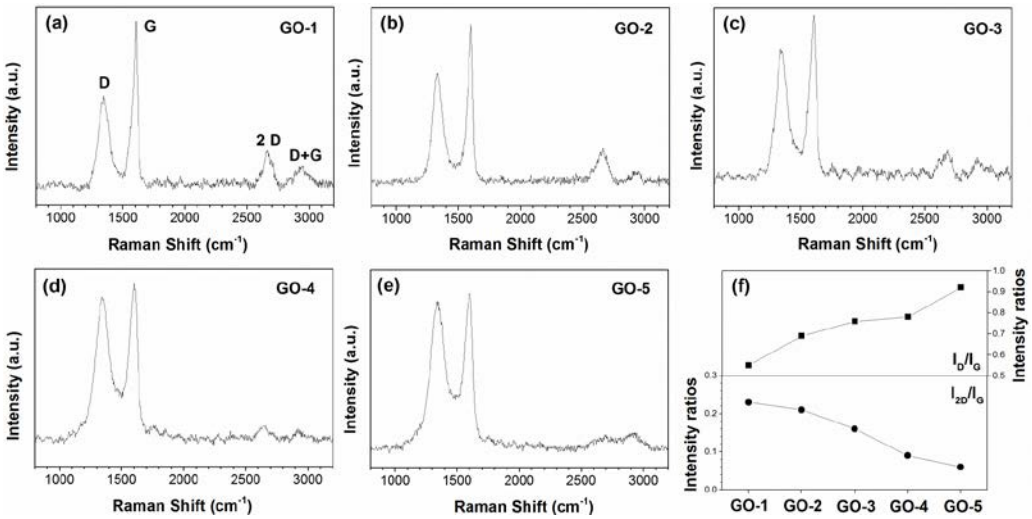

Figure 3: Raman spectra of GO-1 (a), GO-2 (b), GO-3 (c), GO-4 (d) and GO-5 (e); ratios of I_D/I_G and I_{2D}/I_G (f).

3.2 Dispersion of GO sheets

Chemical functionalization of GO or graphene can facilitate uniform dispersion and enhance the interfacial interaction with epoxy matrices. The oxygen-containing groups on GO, such as epoxy, carboxyl and ketone groups, can react with amine compounds under mild condition. Therefore, GO powders (0.2 wt%) were firstly dispersed in curing agent IPDA by sonication and magnetic stirring at 90 °C for 6 h. The dispersion states of GO in IPDA were observed by optical microscope (Fig.4a-e). As can be seen, the oxidation degree has a significant impact on the dispersibility of GO in IPDA. GO-1 tends to significantly agglomerate due to the low content of oxygen-containing groups and high proportions of graphitic carbon. As the oxidation level increases, the dispersibility of GO shows a distinct improvement up to GO-4, whereas GO-5 shows clear agglomeration again. This is because the covalent bonding between GO and IPDA would contribute to uniform dispersion of GO, but the high oxidation degree and hydrogen content of GO-5 may cause a robust agglomeration through hydrogen bonding and dipolar interaction between GO sheets. To further demonstrate the miscibility between GO and IPDA, the status GO/IPDA blends were observed after standing for one week. As shown in Fig. 4f, GO-1 and GO-5 clearly settle down, while GO-2, GO-3 and GO-4 retain visually uniform dispersion in IPDA. Taking the low oxidation degree and worst dispersibility into account, GO-1 is excluded in the following study.

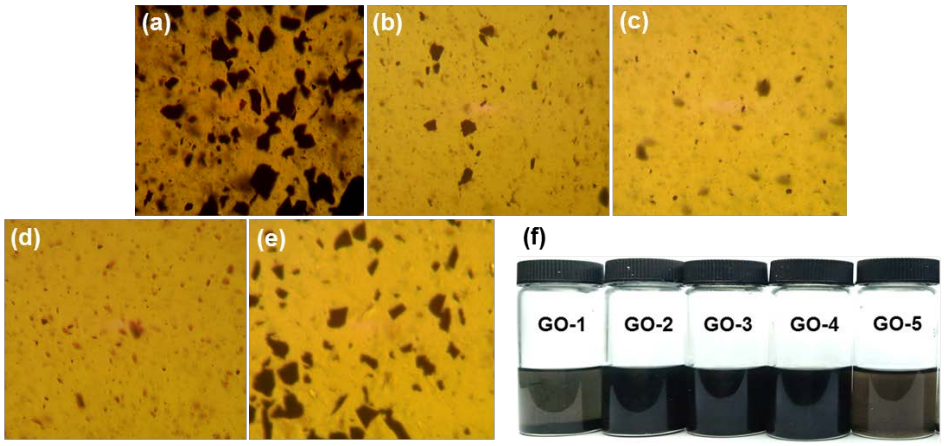

Figure 4: Optical micrographs (magnification = 200) of IPDA/GO mixtures before curing: GO-1 (a), GO-2 (b), GO-3 (c), GO-4 (d) and GO-5 (e); photographs of IPDA/GO mixtures after standing one week.

In order to confirm the chemical functionalization of GO during the dispersion process, the structures of GO in the obtained blends (abbreviated as F-GO) were studied by XPS and FTIR spectroscopy. F-GO powders were obtained by diluting the blend of GO and IPDA (Fig. 4f) with acetone, followed by filtration and washing with excessive acetone. As a representative, Fig. 5 shows the survey and high-resolution N1s XPS spectra of F-GO-4. The survey of F-GO-4 (Fig. 5a) show the presence of N1s signal and the nitrogen content is 9.9 at%, indicating that the surface of GO-4 has been functionalized by IPDA. High-resolution N1s XPS spectrum (Fig. 5b) can be deconvoluted into four types of nitrogen peaks, including C=N (~398.5 eV), C-N (~399.3 eV), O=C-N (~400.9 eV), and C-NH_3^+ (~401.9 eV). FTIR spectroscopy provides a further understanding of the bonding chemistry between GO and IPDA. In the FTIR spectrum of F-GO-4 (Fig. 5c), the carbonyl (~1720 cm^{-1}) and epoxy (1155 cm^{-1}) bands almost disappear in comparison with the spectrum of GO-4. The band at 1640 cm^{-1} can be assigned to the overlap of C=N and C=O stretching vibrations in imine and amide groups, respectively. The bands at 1585 and 1209 cm^{-1} are related to C-N-H bending vibration and C-N stretching vibration in amide groups. According to the results of XPS and FTIR spectroscopy, it can be concluded that the ketone, carboxyl and epoxy groups on GO reacted with IPDA through Schiff base and nucleophilic substitution reactions.

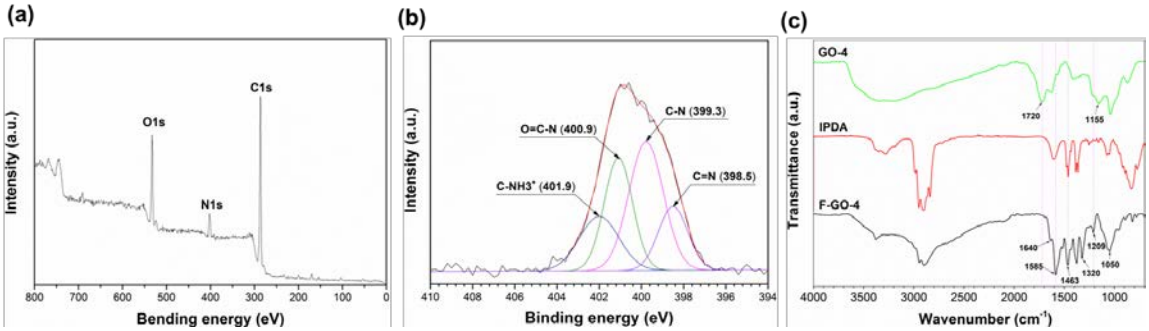

Figure 5: The survey (a) and high-resolution (b) N1s XPS spectra of F-GO-4; FTIR spectra of GO-4, IPDA and F-GO-4 (c).

3.4 Mechanical properties

Tensile and fracture toughness tests were performed to invetigate the reinforcing effects of GO with different oxidation degree. The results of mechanical tests are shown in Fig. 6. Low filler loading (0.2 wt%) was selected in this study to well distinguish the difference in dispersibility of various GO.. As can be seen, the mechianical propeties of resluting composites are indeed affected by the oxidation degree of GO fillers. GO-4 shows the best reinforcing effects on both tensile property and fracture toughness. This is because the reinforcing effects of GO depend heavily on the dispersion state and interfacial interaction between GO and epoxy matrix. GO-4 shows the best dispersibility among five GO samples, and the high content of oxygen-containing groups (ketone, carboxyl and epoxy groups) would contribute to robust interfical interactions with epoxy matrix through covalent bonding. Although GO-5 has the highest oxygen content, it shows little impact on the mechanical properties of epoxy matrix due to the poor dipseribility. The addtion of GO-4 gives about 16 and 6% increase in tensile strength and Young's modulus in comparision of neat epoxy resin. Compared with tensile properties, GO fillers show a more significant impact on the fracture toughenss of epoxy matrix. The composite with GO-4 shows about 56 and 128% increase in the critical stress intensity factor (K_{IC}) and the critical strain energy release rate (G_{IC}), respectively. The toughening mechanisms of epoxy/GO composites generally involve crack deflection, crack pinning and debonding effects.

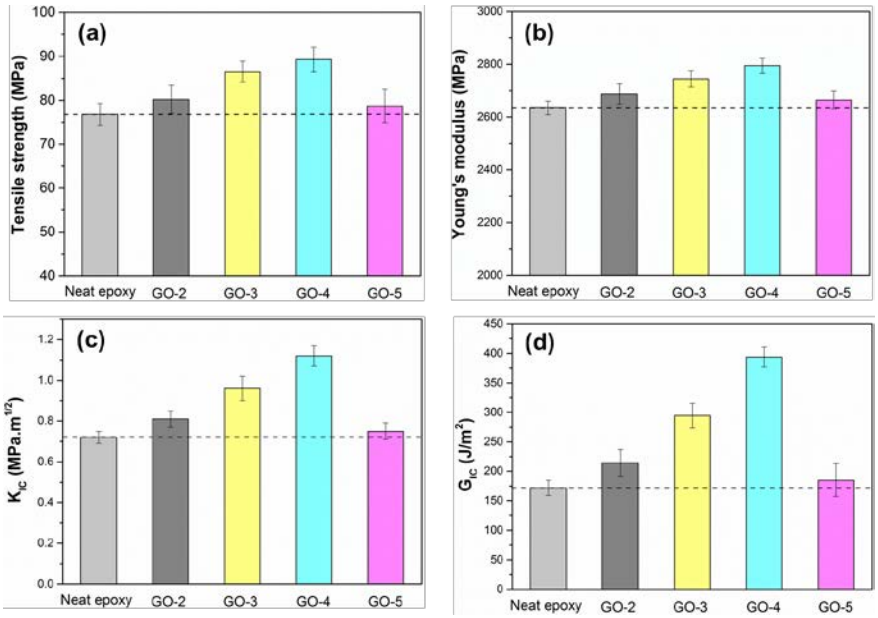

Figure 6: Tensile strength (a), Young's modulus (b) and fracture toughness (c and d) of neat epoxy resin and the composites.

SEM fractography was performed to study the fracture behaviors of neat epoxy and the composites (Fig. 7). The neat epoxy sample shows relatively smooth crack surfaces with river-like patterns (Figs. 7a-c), which is a typical brittle failure mode. In sharp contrast, the fracture surfaces of epoxy/GO-4 composite are much rougher and shows a large number of tortuous cracks (Figs. 7d-f), which indicates more energy was dissipated during crack propagation and leads to increased toughness. Unlike epoxy/pristine graphene composite in our previous study, debonded GO-4 can be rarely observed from the fracture surfaces. This suggests a robust interfacial interaction between GO-4 and epoxy matrxi due to the cobalent bonding. It should be noted that although epoxy/GO-5 composite show rough fracture surfaces (Figs. 8g-h), aggregations of GO-5 can be observed with great possibility (Fig. 8h). These aggregations can cause stress concentration and deteriorate the mechanical performance of epoxy matrix.

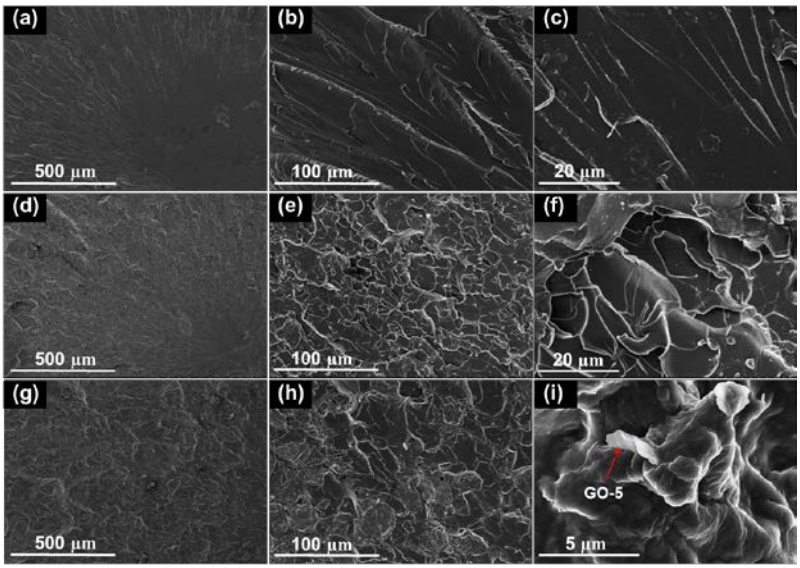

Figure 7: SEM micrographs of fractured surfaces of neat epoxy resin (a-c), epoxy/GO-4 (d-f) and epoxy/GO-5 (g-i) composites at low and high magnification.

3.5 Thermo-mechanical properties

Thermo-mechanical properties of neat epoxy and epoxy/GO composites were investigated by DMA. Fig. 8 shows the storage modulus, loss modulus and loss factor (tan δ) versus temperature plots,. Storage modulus, an index to reflect the elastic properties, is distinctly influenced by the interficial interaction between reinforcing filler and resin matix for polymer composites. Compared with neat epoxy, all the composites show increased storage modulus values in the glassy region (Fig. 8a). Notably, the epoxy/GO-4 composite shows the maxium storage modulus value of 2803 MPa (at 25 °C), which is ~9% higher than that of neat epoxy resin. The increase in storage modulus is because the covalent bonding between GO and epoxy matrix can restrict the mobility of polymer chain at room temperature.

The loss modulus can reflect the energy dissipated as heat due to the internal friction of polymer chains. As can be seen in Fig. 8b, the incoporation of GO deacreses the onset temperature of polymer chain motion and increases the maximun value of loss moludus. This is because IPDA funcitonlized GO can participate in the curing reaction, and decrease the crossliking density of epoxy network as discussed in DSC study, resulting in the increased mobility of the polymer chains in the glasstransition process. In addition, the incorporation of GO may provide additional internal friction between GO and polymer chains.

The temperature at the maximum tan δ value (the ratio of loss modulus to storage modulus) is often taken as glass-transition temperature (T_g). All the composites show lower T_g values compared with that of neat epoxy due to their lower crosslinking density (Fig. 8c). The T_g value of neat epoxy is 145.7 °C, and epoxy/GO-4 composite shows the lowest T_g value of 132.2 °C. There exist controversial

results with regart to the effects of incorporation of functionalized graphene on the T_g values of epoxy composites. Many researchers claimed that graphene filler could restrict the mobility of the polymer chains by covalent bonding, leading to an increase in T_g value. On the other hand, the incorporation of graphene filler may disturb the curing reactions and decrease the crosslinking density of epoxy matrix. In this work, the second effect seems to play a dominate role to determin the T_g values for epoxy/GO composites.

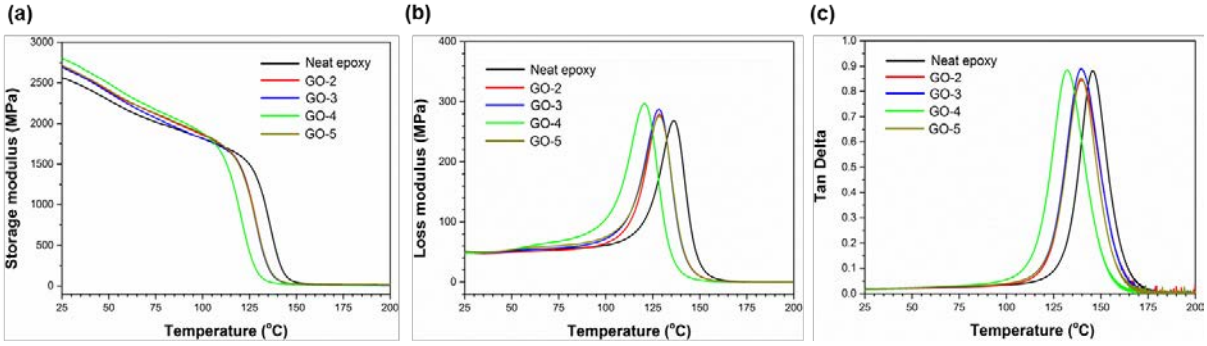

Figure 8: Storage modulus (a), loss modulus (b) and tan δ (c) versus temperature curves of neat epoxy and the epoxy/GO composites

4 CONCLUSIONS

In summary, GO powders with different oxidation degree have been sucessfully prepared through a modified Hummers'method by varying the oxidation conditions. With increasing the oxidation time and the amount of oxidant, the oxygen and hydrogen contents of GO show a gradual increase. The results of XPS and FTIR spectroscopy measurements indicate carbonyl, carboxylic and phenolic groups formed at the early stage for the oxidation of graphite. As the oxidation developed, ether/epoxy and aliphatic hydroxyl groups gradually become dominant at the surfaces of GO. The surfaces of GO can be conviently functionalized by amine hardener (IPDA) *via* Schiff-base and nucleophilic substitution reactions during the dispersion process. Microscopic observations indicate that the GO samples with the lowest (GO-1) and highest (GO-5) oxidation degree show clear aggregates in the epoxy matrix. The results of mechanical tests indicate that the reinforcing effects of different GO on the epoxy matrix vary greatly, especially for the fracture toughness. Among five GO samples, GO-4 shows the best ability in toughening the epoxy matrix due to its superior dispersibility and interfacial interactions. The incorporation of only 0.2 wt% GO-4 can give 56 and 128% enhancement in K_{IC} and G_{IC}, respectively. Finally, DMA measurement indicates the incorporation of GO would decrease the crosslinking density of epoxy matrix and result in the decreased T_g values.

REFERENCES

[1] R. Auvergne, S. Caillol, G. David, B. Boutevin, J.P. Pascault, Biobased Thermosetting Epoxy: Present and Future, *Chem Rev* 114(2) (2014) 1082-1115.
[2] N. Domun, H. Hadavinia, T. Zhang, T. Sainsbury, G.H. Liaghat, S. Vahid, Improving the fracture toughness and the strength of epoxy using nanomaterials - a review of the current status, Nanoscale 7(23) (2015) 10294-10329.
[3] S.C. Kunz, J.A. Sayre, R.A. Assink, Morphology and toughness characterization of epoxy resins modified with amine and carboxyl terminated rubbers, Polymer 23(13) (1982) 1897-1906.
[4] A.F. Yee, R.A. Pearson, Toughening Mechanisms in Elastomer-Modified Epoxies .1. Mechanical Studies, J Mater Sci 21(7) (1986) 2462-2474.
[5] R. Bagheri, B.T. Marouf, R.A. Pearson, Rubber-Toughened Epoxies: A Critical Review, Polym Rev 49(3) (2009) 201-225.
[6] X.Z. Song, S.X. Zheng, J.Y. Huang, P.P. Zhu, Q.P. Guo, Miscibility, morphology and fracture toughness of tetrafunctional epoxy resin/poly (styrene-co-acrylonitrile) blends, J Mater Sci 35(22) (2000) 5613-5619.

[7] S.X. Zheng, J.A. Wang, Q.P. Guo, J. Wei, J.A. Li, Miscibility, morphology and fracture toughness of epoxy resin poly(styrene-co-acrylonitrile) blends, Polymer 37(21) (1996) 4667-4673.
[8] Z.K. Zhong, S.X. Zheng, J.Y. Huang, X.G. Cheng, Q.P. Guo, J. Wei, Phase behaviour and mechanical properties of epoxy resin containing phenolphthalein poly(ether ether ketone), Polymer 39(5) (1998) 1075-1080.
[9] B. Francis, S. Thomas, G.V. Asari, R. Ramaswamy, S. Jose, V.L. Rao, Synthesis of hydroxyl-terminated poly(ether ether ketone) with pendent tert-butyl groups and its use as a toughener for epoxy resins, J Polym Sci Pol Phys 44(3) (2006) 541-556.
[10] B. Zewde, P. Pitliya, A. Karim, D. Raghavan, Synergistic Effect of Functionalized Carbon Nanotubes and Micron-Sized Rubber Particles on the Mechanical Properties of Epoxy Resin, Macromol Mater Eng 301(5) (2016) 542-548.
[11] D. Carolan, A. Ivankovic, A.J. Kinloch, S. Sprenger, A.C. Taylor, Toughening of epoxy-based hybrid nanocomposites, Polymer 97 (2016) 179-190.
[12] B.B. Johnsen, A.J. Kinloch, R.D. Mohammed, A.C. Taylor, S. Sprenger, Toughening mechanisms of nanoparticle-modified epoxy polymers, Polymer 48(2) (2007) 530-541.
[13] K. Wang, L. Chen, J.S. Wu, M.L. Toh, C.B. He, A.F. Yee, Epoxy nanocomposites with highly exfoliated clay: Mechanical properties and fracture mechanisms, Macromolecules 38(3) (2005) 788-800.
[14] F.H. Gojny, M.H.G. Wichmann, B. Fiedler, K. Schulte, Influence of different carbon nanotubes on the mechanical properties of epoxy matrix composites - A comparative study, Compos Sci Technol 65(15-16) (2005) 2300-2313.
[15] G. Zhang, J. Karger-Kocsis, J. Zou, Synergetic effect of carbon nanofibers and short carbon fibers on the mechanical and fracture properties of epoxy resin, Carbon 48(15) (2010) 4289-4300.
[16] M.A. Rafiee, J. Rafiee, Z. Wang, H.H. Song, Z.Z. Yu, N. Koratkar, Enhanced Mechanical Properties of Nanocomposites at Low Graphene Content, ACS nano 3(12) (2009) 3884-3890.
[17] Y.J. Wan, L.C. Tang, L.X. Gong, D. Yan, Y.B. Li, L.B. Wu, J.X. Jiang, G.Q. Lai, Grafting of epoxy chains onto graphene oxide for epoxy composites with improved mechanical and thermal properties, Carbon 69 (2014) 467-480.
[18] Y.T. Park, Y.Q. Qian, C. Chan, T. Suh, M.G. Nejhad, C.W. Macosko, A. Stein, Epoxy Toughening with Low Graphene Loading, Adv Funct Mater 25(4) (2015) 575-585.
[19] Y.W. Zhu, S. Murali, W.W. Cai, X.S. Li, J.W. Suk, J.R. Potts, R.S. Ruoff, Graphene and Graphene Oxide: Synthesis, Properties, and Applications, Adv Mater 22(35) (2010) 3906-3924.
[20] D.R. Dreyer, S. Park, C.W. Bielawski, R.S. Ruoff, The chemistry of graphene oxide, Chem Soc Rev 39(1) (2010) 228-240.
[21] D.R. Bortz, E.G. Heras, I. Martin-Gullon, Impressive Fatigue Life and Fracture Toughness Improvements in Graphene Oxide/Epoxy Composites, Macromolecules 45(1) (2012) 238-245.
[22] Z. Li, R.G. Wang, R.J. Young, L.B. Deng, F. Yang, L.F. Hao, W.C. Jiao, W.B. Liu, Control of the functionality of graphene oxide for its in epoxy nanocomposites application, Polymer 54(23) (2013) 6437-6446.
[23] L. Chen, S.G. Chai, K. Liu, N.Y. Ning, J. Gao, Q.F. Liu, F. Chen, Q. Fu, Enhanced Epoxy/Silica Composites Mechanical Properties by introducing Graphene Oxide to the Interface, ACS applied materials & interfaces 4(8) (2012) 4398-4404.
[24] Q.H. Liu, X.F. Zhou, X.Y. Fan, C.Y. Zhu, X.Y. Yao, Z.P. Liu, Mechanical and Thermal Properties of Epoxy Resin Nanocomposites Reinforced with Graphene Oxide, Polym-Plast Technol 51(3) (2012) 251-256
[25] T. Jiang, T. Kuila, N.H. Kim, B.C. Ku, J.H. Lee, Enhanced mechanical properties of silanized silica nanoparticle attached graphene oxide/epoxy composites, Compos Sci Technol 79 (2013) 115-125